

High-Pressure Electrudes: The Chemical Nature of Interstitial Quasiatoms

Mao-sheng Miao^{*,†,§} and Roald Hoffmann^{*,‡}

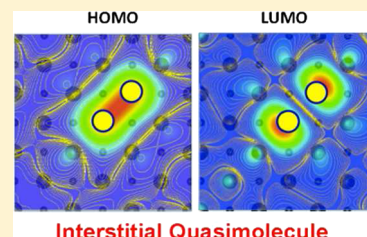
[†]Department of Chemistry and Biochemistry, California State University, Northridge, California 91330, United States

[§]Beijing Computational Science Research Center, Beijing 10084, P. R. China

[‡]Department of Chemistry & Chemical Biology, Cornell University, Ithaca, New York 14853, United States

S Supporting Information

ABSTRACT: Building on our previous chemical and physical model of high-pressure electrudes (HPEs), we explore the effects of interaction of electrons confined in crystals but off the atoms, under conditions of extreme pressure. Electrons in the quantized energy levels of voids or vacancies, interstitial quasiatoms (ISQs), effectively interact with each other or with other atoms, in ways that are quite chemical. With the well-characterized Na HPE as an example, we explore the ionic limit, ISQs behaving as anions. A detailed comparison with known ionic compounds points to high ISQ charge density. ISQs may also form what appear to be covalent bonds with neighboring ISQs or real atoms, similarly confined. Our study looks specifically at quasimolecular model systems (two ISQs, a Li atom and a one-electron ISQ, a Mg atom and two ISQs), in a compression chamber made of He atoms. The electronic density due to the formation of bonding and antibonding molecular orbitals of the compressed entities is recognizable, and a bonding stabilization, which increases with pressure, is estimated. Finally, we use the computed Mg electrude to understand metallic bonding in one class of electrudes. In general, the space confined between atoms in a high pressure environment offers up quantized states to electrons. These ISQs, even as they lack centering nuclei, in their interactions with each other and neighboring atoms may show anionic, covalent, or metallic bonding, all the chemical features of an atom.



The electronic density due to the formation of bonding and antibonding molecular orbitals of the compressed entities is recognizable, and a bonding stabilization, which increases with pressure, is estimated. Finally, we use the computed Mg electrude to understand metallic bonding in one class of electrudes. In general, the space confined between atoms in a high pressure environment offers up quantized states to electrons. These ISQs, even as they lack centering nuclei, in their interactions with each other and neighboring atoms may show anionic, covalent, or metallic bonding, all the chemical features of an atom.

INTRODUCTION

Electrudes are materials in which some electrons occupy void spaces instead of being specifically attached to atoms. Though one could trace them back to Humphry Davy's discovery of alkali metal–ammonia solutions over 200 years ago,¹ they were firmly established in chemistry in Jim Dye's work in recent decades,² and subsequently found in a number of materials, including inorganic and organometallic ones.^{3–7} And, more recently, electrudes have been observed and calculated in materials under high pressure, in some quite simple atomic compositions, even elemental ones.^{8–21} That the electrons in a way play the role of atomic anions in these materials is widely believed,^{9,12,16–20,22–25} hence the electrude name. Rousseau and Ashcroft have constructed an informative model for HPEs, of electrons moving freely in the space between periodically arranged, variable size impenetrable spheres.²⁶

In recent work, we showed the importance of the quantum nature of the electrons occupying compressed interstitial space in crystals, which led us to a theory for the occurrence of high-pressure electrudes (HPEs).²⁷ The space confined by surrounding atoms carries with it quantized energy states, orbitals. The energy of these orbitals (strictly speaking, of the electrons occupying them) naturally increases with external pressure, because the interstitial volume diminishes. So does the energy of the outermost electrons of any pressure-confined atom, and, for reasons of orthogonality to core electrons, the rise in energy with pressure of the electrons in atomic orbitals may be more drastic than that of the electrons in voids. Under sufficiently high

pressure, electrons may then move to occupy the quantized orbitals of interstitial space rather than the atomic orbitals. In the process, interstitial quasiatoms (ISQs) are formed, yielding HPEs. A further gain in stability obtains from the electrostatic interaction of negatively charged ISQs and atom-based cations.

In this work, we will further explore the nature of the ISQs, especially their similarity (or lack thereof) to real anions. The potential formation of chemical bonds between ISQs or between an ISQ and a real atom will be examined. And so will the delocalization of ISQs, in low-dimensional and three-dimensional arrays.

RESULTS AND DISCUSSION

ISQs are negatively charged. It is obvious to draw an analogy between them and inorganic anions in ionic compounds, and this connection has been made in the literature.^{9,12,16–19,22–24} We proceed to analyze one ionic HPE case in detail, and make the analogy substantive.

Sodium, an Ionic HPE. As both predicted by theory and observed in experiment, HPE Na crystallizes in the Ni₂In structure¹² at about 200 GPa, the Na atoms occupying the Ni sites and the ISQs in the In sites. The structure is also known as double hexagonal close packed (DHCP), and is shown in Figure 1.

Received: January 8, 2015

Published: February 23, 2015

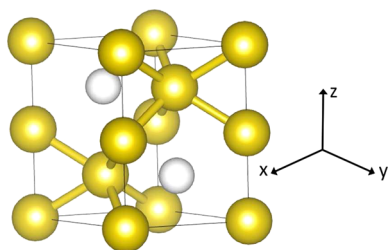


Figure 1. Na HPE structure at 200 GPa. The yellow balls show the position of the Na cores, the lines are nearest neighbor contacts. The white balls indicate the centers of the ISQs.

We would like to have a feeling for the electron density at an ISQ. The electron density that emerges from a VASP calculation can be analyzed with the help of Bader's Quantum Theory of Atoms In Molecules (QTAIM) scheme.²⁸ In this method charge basins and the boundaries between them are obtained from a computation of the gradient of the density. If there is a concentration of electron density in a void, off the atomic sites, it will act as an attractor, and a basin will be defined around it. Figure 2 shows the computed atomic and ISQ basins that result for Na at 300 GPa.

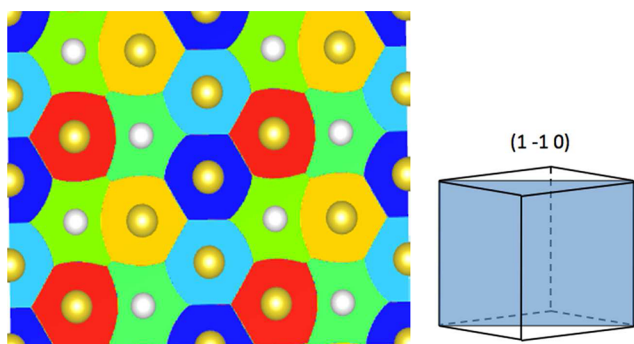


Figure 2. Calculated Bader basins for HPE Na at 300 GPa. The Bader basins are presented on the (1 -1 0) lattice plane as shown in the figure. The ISQ basins are in green. In order to show distinctly the boundaries between different Bader basins, we use different colors for all the Na atoms, even if they are equivalent in the crystal structure.

It is then possible to integrate the electron density in that basin, effectively the ISQ. If we do this for Na as a function of pressure, the Bader electron density of the ISQ increases from 0 at 1 atm rapidly to values larger than 0.8 at ~ 100 GPa and then saturates at values of ~ 1.12 electrons above 200 GPa (see Supporting Information (SI) for the full curve). Dong et al., in a similar analysis, calculated the Bader charge in the Na electride as -1.073 at 200 GPa and -1.155 at 500 GPa.²³

It is interesting to correlate the ISQ density with that of an atom-centered anion. The Bader charge is usually significantly smaller than the nominal ionic charge; for example, at $P = 1$ atm, the Bader charge of the chloride ion in NaCl is only -0.78 . In MgO, crystallizing in the rock salt structure, the Bader charge on the oxide is -1.74 . The Na ISQ density in its region of stability is thus in-between 1 and 2 electrons.

The compounds Na_2E ($\text{E} = \text{O}, \text{S}, \text{Se}, \text{Te}$) are interesting in this context. These extended systems assume the antifluorite structure at $P = 1$ atm.²⁹ Not all have been studied theoretically or experimentally at elevated pressures, but it is known that Na_2S in fact takes on the Ni_2In structure under pressures higher than 16 GPa,³⁰ and so does Na_2Te .³¹ This allows a natural comparison

between the Na HPE and a real ionic substance. Table 1 shows the Bader charges and volumes for the Na ISQ and for the Na^+ and E^{2-} ions in Na_2E at selected pressures.

Table 1. Bader Charges and Basin Volumes at Selected Pressures^a

	Bader charge of anion or ISQ (au)	volume (\AA^3)	
		Na^+	anion or ISQ
Na HPE, 300 GPa	-1.12	4.86	3.58
Na_2S , 16 GPa	-1.44	6.32	19.72
Na_2S , 300 GPa	-1.38	4.45	12.64
Na_2Se , 300 GPa	-1.32	4.52	14.15

^aThe Bader analysis separates all space into basins following the gradient of the electron density. Integration of the electron density and space inside the basins leads to the charges and volumes listed.

The Bader charges of the anions are somewhat larger in magnitude than that of the ISQ. The great differential between the ISQ and the real anions is in their volumes. The Na ISQ basin is quite small, somewhat smaller than the Na basin, and much smaller than the S^{2-} or Se^{2-} . So there is a much greater charge density (electrons/volume) in the ISQ than in corresponding real anions. The similarity of the volumes of the interstitial and Na^+ was also noted in a recent study on Na_2He .^{23,32}

We can gain further insight into the nature of the ISQ by projecting the total density of states (DOS) of the HPE Na onto atomic orbitals of Na and ISQ, classified by their angular momentum. To do this projection we need to specify a sphere; we chose its radius to fit the Na and ISQ volumes at 300 GPa ($r_{\text{Na}} = 1.05 \text{ \AA}$, $r_{\text{ISQ}} = 1.00 \text{ \AA}$). The results are shown in Figure 3. Note that the projections distinguish s and p states (1s and 1p) of the ISQ.

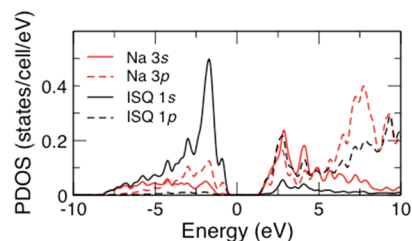


Figure 3. Projected density of states (PDOS) of HPE Na at 300 GPa. The states are projected on spheres centered on Na and ISQ center, radii as specified in the text.

The band gap, characteristic of HPEs, is striking. The valence band, seemingly broad, but actually quite narrow given the pressure, is primarily ISQ 1s. The conduction band is a mixture of Na 3s, 3p and ISQ 1p.

We have tried to gain some further insight into the way the different ISQ orbitals contribute, by looking at the composition of the wave functions of the system at one point in reciprocal space, Γ , and for three specific bands at that point, the highest occupied crystal band (ν_1 , ν for valence) and the three lowest unoccupied states (in bands c_1 , c_2 , and c_3 , c for conduction). Given the relatively flat bands around the Fermi level in the HPE, a single k point may give us a reasonable idea of the overall electron distribution. In ν_1 the ISQ accounts for more than 60% of the density, while c_1 , c_2 , and c_3 at Γ contain large ISQ 1p contributions, amounting to 40%, 50%, and 50%, respectively.

$1p_z$ contributes mainly to c_1 , while c_2 and c_3 consist mainly of $1p_x$ and $1p_y$.

Still another way to see these frontier orbitals of the ZPE is to look at the electron densities in each at Γ , as shown in Figure 4.

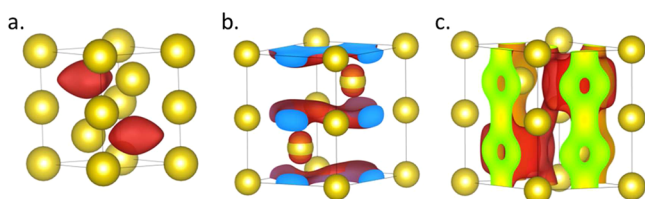


Figure 4. Densities of the highest occupied v_1 (a) and lower unoccupied, c_1 (b) and c_2 (c) crystal orbitals at the Γ point for HPE Na in Ni_2In structure at 300 GPa.

Although the v_1 state consists predominantly of the ISQ $1s$ orbital, it deviates somewhat from spherical symmetry, as expected, reflecting the nonspherical surrounding of the ISQ. The c_1 state, mostly ISQ $1p_z$ in character, overlaps strongly with the $1p_z$ orbitals from the neighboring ISQs, forming two-dimensional layers of electron density. The c_2 state, to which ISQ $1p_x$ and $1p_y$ orbitals contribute, is more localized.

One note in conclusion here: the ISQ $1s$ - $1p$ transition, which is a reasonable way to describe the lowest electronic excitation of compressed Na, is similar to one of the transitions that contribute to the characteristic blue color of alkali metal solutions in anhydrous ammonia, as modeled classically by Jortner.³³

While the previous analysis is on a real material, what follows, a delineation of the ability of ISQs to form chemical bonds with each other and with other atoms, is speculative. We begin by a brief description of the computational model used.

The He Compression Chamber. Our model for the compression of atoms or ISQs is a 108-atom supercell of the face-centered cubic (fcc) He lattice, compressed over the pressure range of $P = 1$ atm to 500 GPa. The lattice constants of the model match well the known equation of state of solid He. To model a compressed atom, the central He of this cell is replaced by the atom; to model an ISQ, the central He is removed, and an O_h constraint is applied to the relaxation, to ensure that the void is not obliterated. Further details may be found in our previous work;²⁷ the computational methodology is detailed in the Theoretical Methods section at the end of this paper.

Chemical Bonds between ISQs. Our previous work showed that while $1p$ and $1d$ orbitals were characteristic of ISQs, realistically only the $1s$ orbital of ISQ was at low enough energy to accommodate electrons originally resident on lattice atoms. Could one then imagine chemical bonding between two ISQs, call them each E, analogous to that between two hydrogen atoms? We examined this possibility by clearing two voids in the He lattice, as close to each other as possible, and as far away as could be (see Figure 5). Given the 108 (106 for the E-E model) atom unit cell constraint, the minimal distance (E-E) between ISQ centers was then 1.70 Å, 1.39 Å at $P = 100$ and 500 GPa, while the maximal distance was 5.10 and 4.17 Å, respectively.

In this Article, we do not relax (at any given pressure) the geometry for the He lattice models but fix them at the structure of ideal He lattice at that pressure. Relaxation, of course, may change the size and shape of the ISQ, but we thought we could orient ourselves in the problem by fixing the ISQ positions. Future work will explore geometrical relaxation.

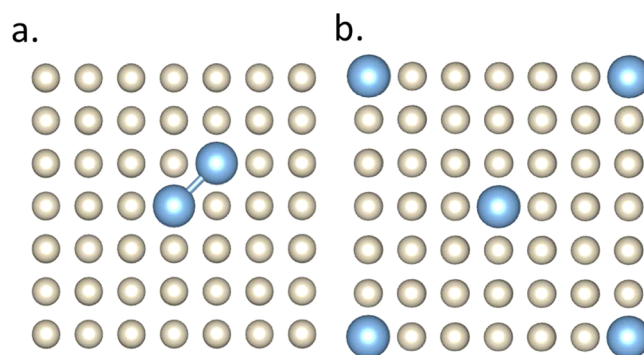


Figure 5. He lattice models containing (a) two adjacent ISQs (E-E) and (b) two reasonably separated ISQs (2E).

We proceed to add two electrons to the system. Figure 6 shows the calculated electron density distribution in the two orbitals of

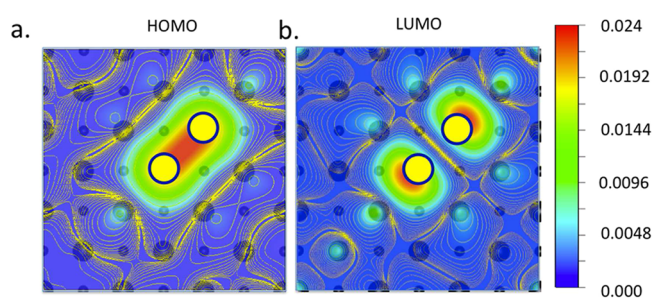


Figure 6. Calculated density of (in units of electrons/ bohr^3) the (a) HOMO and (b) LUMO of an E-E quasimolecule in the He lattice model, at a minimal ISQ separation of 1.70 Å, at 100 GPa. The dark spheres in the background represent the position of He atoms in the fcc lattice; the large spheres represent He atoms in the layer in which the ISQ and other atoms are located, the small spheres the He atoms in the layer below. The two large spheres (blue lines and filled with yellow) close to the center show the positions of the two ISQs. In the following figures, the background spheres (large and small) are always used to represent the He lattice, whereas the large spheres with blue lines and yellow fills represent ISQ positions.

the 100 GPa “minimal” separation model that are most localized on the ISQs. We label these the highest occupied molecular orbital (HOMO) and the lowest unoccupied molecular orbital (LUMO) of a quasimolecule E-E. Note that the LUMO is not actually the lowest unoccupied state of the 106-He-atom model, but is that level which by a projection of the total DOS is most localized on the ISQs (see SI for details).

While we are unable to draw a wave function as such (the plane wave programs do not have atom-based orbitals), the electron densities shown are consistent with a description of the HOMO and LUMO as bonding and antibonding combinations of ISQ $1s$ functions, analogous to the familiar σ_g and σ_u^* MOs of a hydrogen molecule. Note that both HOMO and LUMO of E-E (but especially the LUMO) have some density on the surrounding He atoms; there is some unavoidable coupling with these.

Let us now examine the bonding energy of the E-E molecule and its dependence on external pressure. Within the constraints of our 106-He-atom model, we have only two E-E separations, those shown in Figure 5 as minimal and maximal. So the energies we show correspond to just two points on a hypothetical E-E potential energy plot. We will call the large separation model from now on “2E”, realizing that the separation of the ISQ

centers is particular to the model (5.10Å at 100 GPa, 4.17Å at 500 GPa), and not infinite.

The bonding energy can be calculated by subtracting the energy of an E-E quasimolecule (Figure 5a) from that of the two separated E ISQs (Figure 5b), with two electrons in the system. However, there is a complexity introduced by the He compression model that needs to be addressed. The heliums repel each other; i.e., there is a positive energy contribution from placing two He atoms closer to each other under pressure than their shallow van der Waals minimum. The creation of an isolated ISQ or, in the language of defect chemistry, the creation of a vacancy, will remove 12 nearest-neighbor He-He repulsions per ISQ, or 24 per two separated ISQs. When the two ISQs are placed next to each other, they will only “alleviate” the repulsion of 22 neighboring He atom pairs.

To put it another way, there is an underlying natural stabilization, more relief of He-He repulsive strain, for the separated E than for the small separation E-E pair. That needs to be accounted for in the energetics of E-E formation, and we have done so by calculating the energy difference between 2E and E-E (energy of 2E minus the energy of E-E) for the 106-He-atom model *without* additional electrons. This is called the “strain energy” in Figure 7. The corresponding “total energy” difference

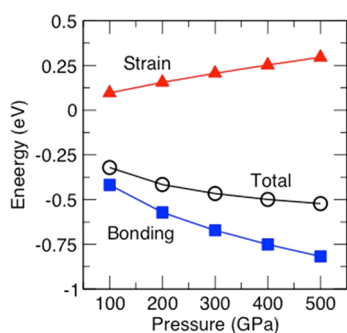


Figure 7. Energy difference between 2E and E-E configurations of two ISQs in the He lattice model.

(for 2 electrons added to the 106-He-atom model) is plotted in Figure 7 as well. We also show the “bonding energy” of the E-E quasimolecule, the total energy minus the strain energy, defined in the same way.

As Figure 7 indicates, the strain relaxation energy (red line) favors the 2E configurations, and increases from 0.1 eV at 100 GPa to 0.3 eV at 500 GPa. After deducting this energy from the total energy (black line), we obtain the bonding energy of the E-E molecule. It is -0.42 eV at 100 GPa. This energy decreases (meaning the E-E quasimolecule becomes more stable) with increasing pressure. At 500 GPa, the bonding energy between two neighboring ISQ becomes -0.82 eV. As the two ISQs come closer under higher pressure, the coupling of their orbitals become stronger, the bonding energy increases in magnitude. The bonding obtained between two ISQs in the model approaches that in a weakly bound diatomic (Li_2 or F_2) at $P = 1$ atm.

Bonding of ISQs with Atoms. ISQs can also form chemical bonds with atoms, if their valence orbital is close in energy to the ISQ orbital, and can overlap with its quantized 1s wave function. As shown in our previous work, below 500 GPa there are only a few atoms whose frontier electrons and orbitals come close in energy to the ISQ orbitals. Among them, we choose Li and Mg

and study the possible bonding interactions between a one-electron ISQ (call it E) and these two atoms.

Li contains one valence electron in its 2s orbital. It can, in principle, form a “chemical bond” with E. Our model for the system consists of a periodic system with a unit cell containing 106 He atoms + one Li + an adjacent vacancy with one electron. Figure 8 shows the density distribution of the two electrons in the

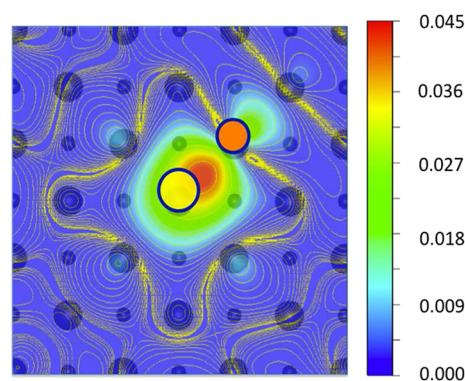


Figure 8. Calculated density (in units of electrons/ bohr^3) of the bonding state of an E-Li quasimolecule in the He lattice model at 100 GPa. Dark spheres mark the positions of He atoms in the lattice (large in-plane, small in plane below). The large light sphere at the center and the medium sphere with orange fill show the positions of the ISQ (E) and the Li atom, respectively.

highest occupied state of this model at 100 GPa. The density, highest between E and the Li atom, clearly looks like that in an E-Li bonding orbital. Note that the Li appears to be using a 2s-2p hybrid in its bonding with the ISQ.³⁴ The corresponding antibonding state mixes with other (He) states in the model and cannot be easily traced.

We need to explore further the properties of the Li-E quasimolecule. Can the bonding of Li with E be characterized as mainly ionic or covalent? We have approached this question in two ways, by comparing the density of Figure 8 with that of a Li-H and Li-Li diatomic in the same compression chamber (Figure 9). The SI shows for comparison the electron density of these

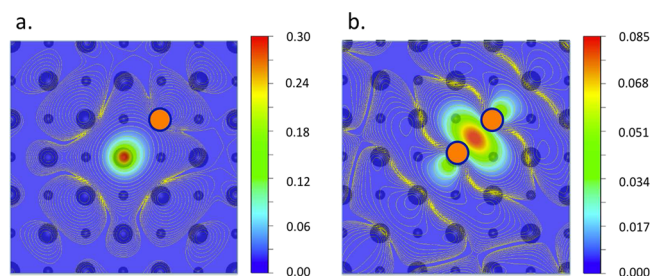


Figure 9. Electron density of the HOMO orbital (in units of electrons/ bohr^3) for (a) Li-H and (b) Li_2 in the 106-He-atom compression chamber at 100 GPa. The large spheres with orange fill show the position of Li atoms. The H atom at left is at the center of the red electron density maximum in the contour plot.

diatomics in vacuum. It appears that the ionically bonded Li-H, with its electron density really concentrated on the hydride, is not that a good model for the Li-E system. Li-Li is better.

We also studied E-Be and E-B interactions using the same He-chamber at 100 GPa. For E-Be, we put two electrons (over the Be 1s core) in the system, to model a covalent or ionic E-Be bond.

The hydrogen analogue would be BeH^+ , a molecule bound by over 3 eV. For E-B, we added one extra electron, for a total of four valence electrons between the B and the ISQ. The electron densities for the HOMO and LUMO orbitals of both cases are shown in Figure 10.

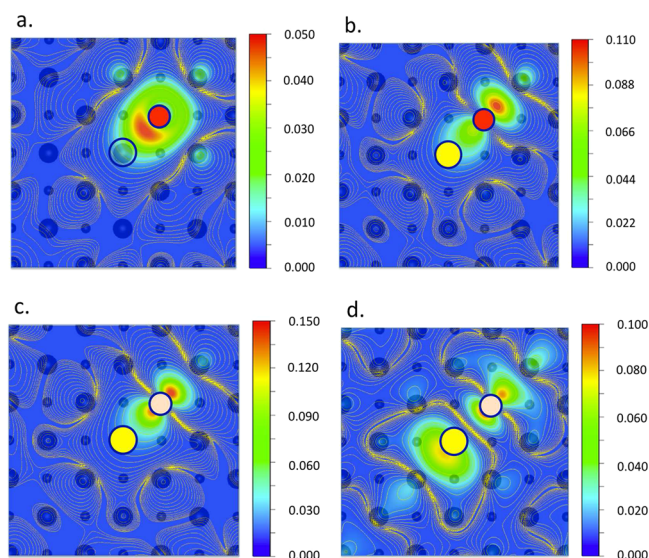


Figure 10. Calculated density (in units of electrons/bohr³) of the (a) HOMO and (b) LUMO of an E-Be quasimolecule in the He lattice model at 100 GPa. Dark spheres mark the positions of He atoms in the lattice (large in-plane, small in plane below); the large sphere at the center and the sphere filled with red color show the positions of the ISQ and the Be atom. (c,d) Similar electron densities for the E-B quasimolecule. Here the sphere with white fill is the B atom core.

The electrons largely locate between E and Be in the HOMO of our EBe model (Figure 10a), characteristic of a moderately ionic bonding orbital. The LUMO (Figure 10b) is also bonding (no node between E and Be, and has much Be 2p character). The Be-E bonding also shows in that the LUMO (a mixture of ISQ 1s and Be 2p_z, where z is the Be-ISQ axis) is at lower energy than the 2p_{x,y} orbitals of Be. The relevant projections are shown in the SI. It is interesting that one could imagine stability for a system with two electrons more; this would effectively be a four-electron (six counting Be 1s) E-Be quasimolecule.

For E-B, the densities of the HOMO and LUMO+1 states (Figure 10c,d; see also projection in SI) are characteristic of bonding and antibonding states between E 1s and B 2p_z. The B 2s is too low in energy to interact with ISQ 1s.

Mg has two 2s electrons that can be involved in forming bonds with neighboring ISQ. We model an MgE₂ quasimolecule by placing an Mg atom and two vacancies plus two electrons into a 105 He atom cell. AB₂ molecules can be linear or bent; MgH₂ is linear.³⁵ Our simplest He-lattice model can only explore MgE₂ quasimolecule with either linear geometry or with a bent angle of 60°, 90° and 120°. We found that the energies of the above bent MgE₂ are about 0.18, 0.89, and 1.82 eV higher than that of the linear quasimolecule at 100 GPa.

Figure 11a,b shows the HOMO−1 and the HOMO states of the model. They are both occupied by two electrons. The densities of these MOs are consistent with those of the lowest (bonding) and middle (nonbonding) MOs of an HMgH or RMgR molecule, sketched in Figure 11c.

In concluding this section we mention a connection of the ideas on ISQs bonding to atoms with related ideas on the

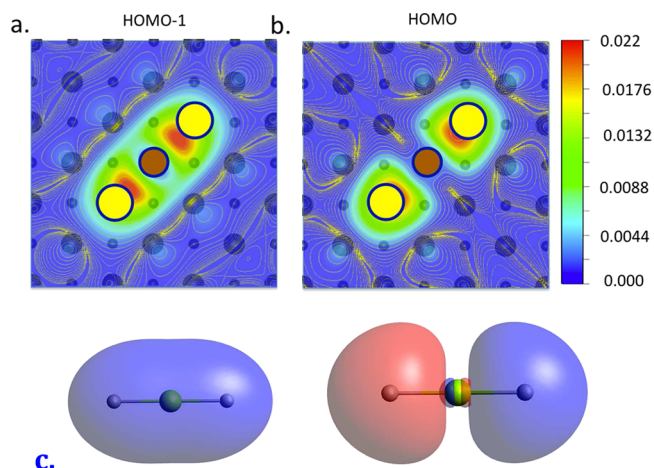


Figure 11. Calculated density of the (a) bonding and (b) nonbonding levels of an MgE₂ quasimolecule in the He lattice model. Dark spheres (large and small) in the background indicate the position of He atoms in the lattice; the two large light spheres close to the center show the positions of the two E ISQs, and the medium-sized brown sphere at the center denotes the position of Mg atom. (c) Schematic contours of wave functions for the two lowest valence MOs of a linear HMgH.

bonding capabilities of atomic clusters, so-called “superatoms”.³⁶ We turn next to networks of ISQs interacting with each other.

Magnesium, a Metallic HPE. The behavior of the ISQs in the HPE phase of Mg is quite different from those in Na. If we assign an ISQ sphere to each region where there is a distinct off-atom electron density, the calculated Mg HPE can be described as Mg(ISQ)₂.¹⁸ As shown in Figure 12, the HPE adopts the MgB₂

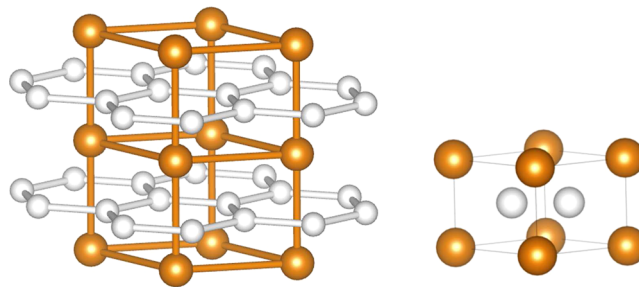


Figure 12. ISQ in the simple hexagonal structure of HPE Mg at 800 GPa. The gold and the white balls represent Mg and ISQ positions, respectively.

structure; the Mg atoms form a simple hexagonal lattice, but there is electron density in the interstices, as shown. Each Mg provides in principle two 2s electrons, and these enter each in one ISQ 1s. The calculated Bader charge in the ISQ basins at 800 GPa is −0.72, close to what one might expect for a full one-electron occupation of each ISQ (cf. −0.78 on Cl in NaCl).

Examination of the electron density in this 800 GPa electricle (Figure 13 in side and top views) shows two-dimensionally delocalized electron density in the planes between the Mg cores. Indeed, the calculations¹⁸ indicate this material is metallic—one can think of it as an overlapping honeycomb lattice of ISQs.

One way to probe bonding between atoms (and ISQs) is through a Crystal Orbital Hamiltonian Population (COHP) analysis.³⁷ For pairs of atoms, COHP examines whether the states in a given energy interval are bonding (negative contribution to total energy), or antibonding. Thus, COHP is an energy-selective way of looking at where there is bonding (or

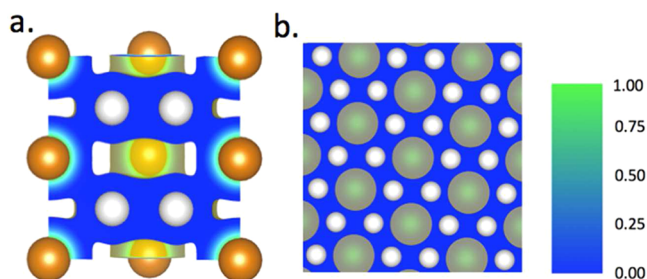


Figure 13. (a) Side view of the electron distribution of simple hexagonal Mg at 800 GPa. (b) Top view of electron density in (002) plane of simple hexagonal Mg at 800 GPa. The gold balls show the positions of the Mg atoms, the white balls the location of the ISQs. The color scale gages the electron density.

antibonding) in a structure. Figure 14 shows the COHP in the Mg electrified phase at 800 GPa.³⁸

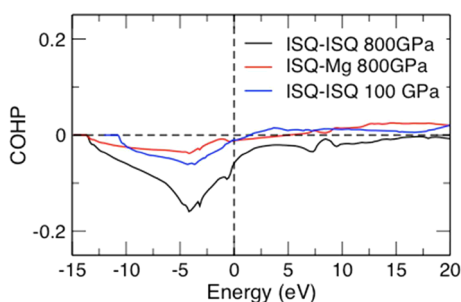


Figure 14. Calculated Crystal Orbital Hamiltonian Population (COHP) for simple hexagonal Mg at 800 GPa. The black and the red lines represent the COHP of ISQ-ISQ and ISQ-Mg. For comparison, we also show the COHP of ISQ-ISQ pair in simple hexagonal Mg at 100 GPa (blue line).

The COHP in Figure 14 indicates a substantial bonding interaction between the ISQs as well as one with the Mg. What kind of bonding is involved here? The integrated COHP up to the Fermi level (ICOHP) is -1.17 eV/cell for ISQ-ISQ pair, compared with the smaller value of -0.32 eV/cell for the ISQ-Mg interaction. The Mg-Mg ICOHP is even smaller. For calibration, the integrated COHP in ($P = 1$ atm) diamond is -6.52 eV (C-C), in rock salt is -0.13 eV (per NaCl pair), and in metallic Fe is -1.65 eV (Fe-Fe). It appears that the ISQ-ISQ bonding in the metallic Mg HPE is partly covalent, partly metallic. We also examined ICOHP values in a classical intermetallic compound, CuZn in a CsCl structure. The ICOHP values range from -0.40 (Cu-Cu) to $+0.27$ eV/pair. Perhaps the HPEs of the Mg type should be called intermetallic.

Relevant to the existence of metallic ISQ interaction in an HPE, we mention the important work of Pickard and Needs,²⁴ who predict for the alkali metals (at fairly low compression) the development of stable ferromagnetic electrified phases.³⁹

CONCLUSIONS

The chemical nature of the electrons entering interstitial sites in high-pressure electrified phases is clarified in this work. Our results show that the enclosed interstitial sites in HPE are chemically comparable to a real atom, which is why we called them ISQs. They contain quantized orbitals that can accommodate electrons. In some cases, those orbitals can accommodate electrons, forming effective anions. They can also form both

covalent and metallic bonds with neighboring interstitials or atoms.

We examine in some detail the HPEs of Na and Mg. These two cases show us the range of electronic behavior available to an ISQ—it can behave simply as an anion, or interact with other ISQs in a type of intermetallic bonding. We use QTAIM in both studies; this allows us to say for Na that the ISQs in this element contain somewhere between 1 and 2 electrons, and behave much like inorganic anions. A comparison to isostructural Na_2X ($\text{X} = \text{Se}, \text{Te}$) reveals the much smaller volume occupied by the ISQ electrons. In the case of Mg we dissect in some detail another option a metallic HPE, with overlapping ISQs.

For further studies, our tool is a compression chamber of 108 He atoms, in the pressure range between 1 atm and 500 GPa. If a vacancy is created in this space, and the surrounding atoms not allowed to collapse it, the resulting energy levels, primarily a 1s level, provide a home for an electron that effectively is atom-like. This is the ISQ. We explore the bonding capabilities of the ISQ, call it E, by placing one or two of these next to a Li or Mg atom confined in the same pressure chamber. Effective quasimolecules E-E, E-Li, and E-Mg-E form. Large splittings between bonding and antibonding states are observed, and a significant bonding energy in each case.

The analogy of HPEs to binary or ternary chemical compounds is not new to us. It may be found in the literature, in the work of Fortov,²² Ma,^{12,16} Pickard and Needs,^{9,19,24} Bergara,¹⁶ Oganov,^{12,23} and their co-workers. We believe that our detailed study establishes and extends the scope of the electrified view of HPEs.

The ISQ acts as a chemical species although it does not contain nuclei and core electrons. At first it sounds surprising that empty space can have all the important features of atoms as chemical species. The key point is the enclosure or the confinement of the space, the effect of pressure, communicated through neighboring atoms. The quantization of the orbitals in ISQs only becomes important when the size of the enclosed space become comparable to the size of typical atoms. Such quasiatoms then initiate in the confined space of a highly pressurized material emergent chemistries.

THEORETICAL METHODS

The geometry and orbital energies in the He lattice model are obtained from density functional calculations using Vienna Ab initio Simulation Package (VASP) code.⁴⁰ The generalized gradient approximation (GGA) within the framework of Perdew–Burke–Ernzerhof (PBE)⁴¹ was used for the exchange–correlation functional, and projector augmented wave (PAW) potentials⁴² were used to describe the ionic potentials. The core radius of He PAW potential is 0.582 Å. The He face centered cubic (FCC) lattice is optimized under a series of pressures from 0 to 500 GPa. A conventional cell (4 atoms) and a k-mesh of $8 \times 8 \times 8$ were used to ensure the convergence of forces and total energies.

A $3 \times 3 \times 3$ supercell model containing 106 He atoms and 2 selected atoms or vacancies (represent ISQ) is used for the calculations under finite pressure. Only 1 k point at the Γ point is used. The atomic positions are not relaxed; the lattice constants are fixed at the constants of He FCC at desired pressure for the supercell model. The cutoff energies vary with the studied atom, but are higher than 600 eV to ensure the convergence of forces on He atoms. For systems that contain excess or insufficient number of electrons, i.e., are charged, a uniform background counter-charge is added to keep the whole supercell neutral. The COHPs are calculated by use of the Stuttgart tight-binding linear muffin-tin orbital (TB-LMTO) code.⁴³

■ ASSOCIATED CONTENT

Supporting Information

Calculated Bader charges in Na HPE as a function of pressure; actual states of the E-E model at various pressures; Li-Li and LiH electron densities in vacuum; actual density of states in the models for Be-E and B-E. This material is available free of charge via the Internet at <http://pubs.acs.org>.

■ AUTHOR INFORMATION

Corresponding Authors

*mmiao@csun.edu

*rh34@cornell.edu

Notes

The authors declare no competing financial interest.

■ ACKNOWLEDGMENTS

M.M. acknowledges the NSF-funded XSEDE resources (TG-DMR130005). Calculations were performed on the Stampede cluster run by the Texas Advanced Computing Center and the computing clusters in the Center for Scientific Computing supported by the CNSI, MRL, and NSF CNS-0960316. The work at Cornell was supported by Efree (an Energy Frontier Research Center funded by the U.S. Department of Energy (Award No. DESC0001057 at Cornell, subcontract to Carnegie Institution of Washington)).

■ REFERENCES

- Zurek, E.; Edwards, P. P.; Hoffmann, R. *Angew. Chem., Int. Ed.* **2009**, *48*, 8198–8232 and references therein. For the related story of the hydrated electron, see: Casey, J. R.; Kahros, A.; Schwartz, B. J. *J. Phys. Chem. B* **2013**, *117*, 14173–14182 and references therein.
- Dye, J. L. *Acc. Chem. Res.* **2009**, *42*, 1564–1572 and references therein. Issa, D.; Dye, J. L. *J. Am. Chem. Soc.* **1982**, *104*, 3781–3782.
- Simon, A. *Coord. Chem. Rev.* **1997**, *163*, 253–270.
- Kim, S. W.; Shimoyama, T.; Hosono, H. *Science* **2011**, *333*, 71–74. Matsuishi, S.; Toda, Y.; Miyakawa, M.; Hayashi, K.; Kamiya, T.; Hirano, M.; Tanaka, I.; Hosono, H. *Science* **2003**, *301*, 626–629.
- Lee, K.; Kim, S. W.; Toda, Y.; Matsuishi, S.; Hosono, H. *Nature* **2013**, *494*, 336–340.
- An excellent case for the role of interstitial electrons in lithium clusters and metal has been made by Goddard and co-workers: (a) McAdon, M. H.; Goddard, W. A., III *Phys. Rev. Lett.* **1985**, *55*, 2563–2566. (b) McAdon, M. H.; Goddard, W. A., III *J. Phys. Chem.* **1987**, *91*, 2607. (c) Li, M.; Goddard, W. A., III *Phys. Rev. B* **1989**, *40*, 12155–12163. (d) Kim, H.; Su, J. T.; Goddard, W. A., III *Proc. Natl. Acad. Sci. U.S.A.* **2011**, *108*, 15101–15105.
- In the F and F' centers of ionic crystals, essentially an electron (or two) is (are) trapped at an anion vacancy at $P = 1$ atm: Hayes, W.; Stoneham, A. M. *Defects and Defect Processes in Nonmetallic Solids*; Wiley: New York, 1985. Stoneham, A. M. *Theory of Defects in Solids*; Clarendon Press: Oxford, 1985.
- Neaton, J. B.; Ashcroft, N. W. *Nature* **1999**, *400*, 141–144. See also: Siringo, F.; Pucci, R.; Angilella, G. G. N. *High Press. Res.* **1997**, *15*, 255–264.
- Pickard, C. J.; Needs, R. J. *Phys. Rev. Lett.* **2009**, *102*, 146401.
- Yao, Y.; Tse, J. S.; Klug, D. D. *Phys. Rev. Lett.* **2009**, *102*, 115503.
- Neaton, J. B.; Ashcroft, N. W. *Phys. Rev. Lett.* **2001**, *86*, 2830–2833.
- Ma, Y.; Eremets, M.; Oganov, A. R.; Xie, Y.; Trojan, I.; Medvedev, S.; Lyakhov, A. O.; Valle, M.; Prakapenka, V. *Nature* **2009**, *458*, 182–185.
- Lazicki, A.; Goncharov, A. F.; Struzhkin, V. V.; Cohen, R. E.; Liu, Z.; Gregoryanz, E.; Guillaume, C.; Mao, H. K.; Hemley, R. J. *Proc. Natl. Acad. Sci. U.S.A.* **2009**, *106*, 6525–6528.
- Gatti, M.; Tokatly, I. V.; Rubio, A. *Phys. Rev. Lett.* **2010**, *104*, 216404.

(15) Marques, M.; Santoro, M.; Guillaume, C. L.; Gorelli, F. A.; Contreras-Garcia, J.; Howie, R. T.; Goncharov, A. F.; Gregoryanz, E. *Phys. Rev. B* **2011**, *83*, 184106.

(16) Rousseau, B.; Xie, Y.; Ma, Y.; Bergara, A. *Eur. Phys. J. B* **2011**, *81*, 1–14.

(17) Pickard, C. J.; Needs, R. J. *Nat. Mater.* **2010**, *9*, 624–627.

(18) Li, P. F.; Gao, G. Y.; Wang, Y. C.; Ma, Y. M. *J. Phys. Chem. C* **2010**, *114*, 21745–21749.

(19) Martinez-Canales, M.; Pickard, C. J.; Needs, R. J. *Phys. Rev. Lett.* **2012**, *108*, 045704.

(20) Zhu, Q.; Oganov, A. R.; Lyakhov, A. O. *Phys. Chem. Chem. Phys.* **2013**, *15*, 7696–7700.

(21) Zurek, E.; Wen, X. D.; Hoffmann, R. *J. Am. Chem. Soc.* **2011**, *133*, 3535–3547.

(22) Maksimov, E. G.; Magnitskaya, M. V.; Fortov, V. E. *Physics—Uspekhi* **2005**, *48*, 761–780.

(23) Dong, X.; Oganov, A. R.; Goncharov, A. F.; Stavrou, E.; Lobanov, S.; Saleh, G.; Qian, G.-R.; Zhu, Q.; Gatti, C.; Zhou, X.-F.; Prakapenka, V.; Konôpková, Z.; Wang, H.-T. *arXiv* **2014**, No. 1309.3827v3.

(24) Pickard, C. J.; Needs, R. J. *Phys. Rev. Lett.* **2011**, *107*, 087201.

(25) This is also true of $P = 1$ atm electrides. See ref 2 and the following for an early description of the electronic structure of Dye's electrides: Singh, D. J.; Krakauer, H.; Haas, C.; Pickett, W. E. *Nature* **1993**, *365*, 39–42. A thorough description of these is given in the following: Dale, S. G.; Otero-de-la-Roza, A.; Johnson, E. R. *Phys. Chem. Chem. Phys.* **2014**, *16*, 14584–14593.

(26) Rousseau, B.; Ashcroft, N. W. *Phys. Rev. Lett.* **2008**, *101*, 046407.

(27) Miao, M.-S.; Hoffmann, R. *Acc. Chem. Res.* **2014**, *47*, 1311–1317.

(28) Bader, R. *Atoms in Molecules: A Quantum Theory*; Oxford University Press: New York, 1994. Bader, R. *Chem. Rev.* **1991**, *91*, 893.

(29) A leading reference to the structural work: Kalarasse, F.; Benecer, B. *Comput. Mater. Sci.* **2011**, *50*, 1806–1810.

(30) Vegas, A.; Grzechnik, A.; Syassen, K.; Loa, I.; Hanfland, M.; Jansen, M. *Acta Crystallogr.* **2001**, *B57*, 151–156.

(31) Beister, H. J.; Klein, J.; Schewe, I.; Syassen, K. *High Press. Res.* **1991**, *7*, 91–95.

(32) The electride interstitial electron volumes computed by Dale et al., ref 25, are larger, but these are at $P = 1$ atm.

(33) Jortner, J. *J. Chem. Phys.* **1959**, *30*, 839–846.

(34) For the involvement of 2p orbitals under pressure, see our previous paper, and the following: Hanfland, M.; Syassen, K.; Christensen, N. E.; Novikov, D. L. *Nature* **2000**, *408*, 174–178. Rousseau, B.; Uehara, K.; Klug, D. D.; Tse, J. S. *ChemPhysChem* **2005**, *6*, 1703–1706.

(35) Shayasteh, A.; Appadoo, D. R. T.; Gordon, I.; Bernath, P. F. *J. Chem. Phys.* **2003**, *119*, 7785–7788. Mg–H in the triatomic is 1.703 Å. Solid MgH₂ takes on the rutile structure.

(36) See references in the following: Luo, Z.; Castleman, A. W. *Acc. Chem. Res.* **2014**, *47*, 2931–2940.

(37) Dronskowski, R.; Blöchl, P. E. *J. Phys. Chem.* **1993**, *97*, 8617–8624.

(38) In the COHP calculation, the Stuttgart TB-LMTO method was used. In this, one usually needs to add empty spheres to avoid the large overlap of the ASA spheres. These are then added at ISQ positions; the calculation of the COHP is then straightforward.

(39) See also: Bergara, A.; Neaton, J. B.; Ashcroft, N. W. *Int. J. Quantum Chem.* **2002**, *91*, 239–244.

(40) Kresse, G.; Furthmüller, J. *Phys. Rev. B* **1996**, *54*, 11169–11186.

(41) Perdew, J. P.; Burke, K.; Ernzerhof, M. *Phys. Rev. Lett.* **1996**, *77*, 3865–3868.

(42) Blöchl, P. E. *Phys. Rev. B* **1994**, *50*, 17953–17979.

(43) Jepsen, O.; Andersen, O. K. *The Stuttgart TB-LMTO Program*, version 47; Max-Planck-Institut für Festkörperforschung: Stuttgart, Germany, 2000; <http://www2.fkf.mpg.de/andersen/>.